Diagn Interv Radiol 2021; 27:308–314

ABDOMINAL IMAGING

ORIGINAL ARTICLE

Radiomics signature as a new biomarker for preoperative prediction of neoadjuvant chemoradiotherapy response in locally advanced rectal cancer

Zhaohe Zhang
Xiran Jiang
Rui Zhang
Tao Yu
Shanshan Liu
Yahong Luo

PURPOSE
Whether radiomics methods are useful in prediction of therapeutic response to neoadjuvant chemoradiotherapy (nCRT) is unclear. This study aimed to investigate multiple magnetic resonance imaging (MRI) sequence-based radiomics methods in evaluating therapeutic response to nCRT in patients with locally advanced rectal cancer (LARC).

METHODS
This retrospective study enrolled patients with LARC (06/2014-08/2017) and divided them into nCRT-sensitive and nCRT-resistant groups according to postoperative tumor regression grading results. Radiomics features from preoperative MRI were extracted, followed by dimension reduction using the minimum redundancy maximum relevance filter. Three machine-learning classifiers and an ensemble classifier were used for therapeutic response prediction. Radiomics nomogram incorporating clinical parameters were constructed using logistic regression. The receiver operating characteristic (ROC), decision curves analysis (DCA) and calibration curves were also plotted to evaluate the prediction performance.

RESULTS
The machine learning classifiers showed good prediction performance for therapeutic responses in LARC patients (n=189). The ROC curve showed satisfying performance (area under the curve [AUC], 0.830; specificity, 0.794; sensitivity, 0.815) in the validation group. The radiomics signature included 30 imaging features derived from axial T1-weighted imaging with contrast and sagittal T2-weighted imaging and exhibited good predictive power for nCRT. A radiomics nomogram integrating carcinoembryonic antigen levels and tumor diameter showed excellent performance with an AUC of 0.949 (95% confidence interval, 0.892–0.997; specificity, 0.909; sensitivity, 0.879) in the validation group. DCA confirmed the clinical usefulness of the nomogram model.

CONCLUSION
The radiomics method using multiple MRI sequences can be used to achieve individualized prediction of nCRT in patients with LARC before treatment.

Colorectal cancer is one of the most common malignancies. It ranks fourth for morbidity and third for mortality among malignant tumors, among which the proportion of rectal cancer with poor prognosis is over 60% (1, 2). Neoadjuvant therapy, combined with total mesorectal excision, has become a common strategy for rectal cancer (3). Response to neoadjuvant chemoradiotherapy (nCRT) is a marker of good prognosis in patients with locally advanced rectal cancer (LARC) (4). Tumor regression grading (TRG) is a reliable biomarker for evaluating the efficacy of nCRT (5, 6). TRG reflects the treatment effect of nCRT by evaluating fibrosis and the ratio of residual tumor cells (4). The accurate nCRT evaluation can only be achieved by postoperative histopathological TRG (3, 4), and there is still no technology that can noninvasively evaluate the therapeutic response.

Magnetic resonance imaging (MRI) is commonly used in the diagnosis, preoperative staging, and therapeutic efficacy evaluation of rectal cancer. Prediction of the efficacy of nCRT by MRI has been rarely reported, partly due to the heterogeneity of the tumor combined with the prevalence of fibrosis and edema of lesions and surrounding tissue after nCRT. Over the recent years, a magnetic resonance TRG system was proposed for the evaluation

From the Department of Medical Imaging (Z.Z., T.Y., Y.L. ✉ *Luoyahong8888@hotmail.com*), and Department of Colorectal surgery (R.Z.), Liaoning Cancer Hospital & Institute, Shenyang, China; Department of Biomedical Engineering (X.J., S.L.), China Medical University, Shenyang, China.

Received 09 January 2020; revision requested 13 February 2020; last revision received 12 May 2020; accepted 18 May 2020.

Published online 6 April 2021.

DOI 10.5152/dir.2021.19677

You may cite this article as: Zhang Z, Jiang X, Zhang R, Yu T, Liu S, Luo Y. Radiomics signature as a new biomarker for preoperative prediction of neoadjuvant chemoradiotherapy response in locally advanced rectal cancer. Diagn Interv Radiol 2021; 27:308–314

of nCRT efficacy by using MRI and evaluating residual tumor and fibrosis. Nevertheless, the magnetic resonance TRG method has a low predictive value for pathological TRG and poor consistency, which hinders its clinical applications (7, 8).

In recent years, radiomics has drawn increasing attention in oncology. Radiomics features selected from medical images have shown to be highly associated with the diagnosis and prognosis of cancers, and even with gene expression patterns (9). Studies highlighted the value of radiomics approaches in determining tumor status, preoperative staging, and efficacy evaluation (9, 10). Nevertheless, the application of the radiomics methods in evaluating therapeutic responses to nCRT is limited (11).

Accordingly, the aim of the present study was to establish an nCRT prediction model based on multiple MRI sequences combined with tumor anatomy and biological characteristics so as to achieve a comprehensive preliminary prediction of nCRT efficacy for rectal cancer before treatment, to provide an essential basis for the rational formulation of clinical diagnosis and treatment decisions, and to avoid unnecessary exposure to radiotherapy and chemotherapy and the related risks such as toxicity and delayed definitive surgery.

Methods

Patients

This retrospective study was approved by the ethics committee of Liaoning Cancer Hospital (No.2018010) and informed consent was waived. Patients with LARC were enrolled between June 2014 and August 2017 from the Department of Radiology of Liaoning Provincial Cancer Hospital. The inclusion criteria were: 1) pathologically confirmed rectal adenocarcinoma (cT3-4 or N+), no distant metastasis; 2) MRI exam before nCRT; 3) no history of anticancer treatments before undergoing MRI and before nCRT; and 4) complete baseline clinical data. The exclusion criteria were: 1) failure to complete nCRT in accordance with the treatment plan; 2) total mesorectal excision not performed after nCRT; or 3) inconsistent scanning equipment or parameters.

Main points

- A radiomics approach based on multiple MRI sequences could be useful to predict the therapeutic response in patients with locally advanced rectal cancer before neoadjuvant chemoradiotherapy.
- A comparison of different machine learning models revealed the random forest model to have the best prediction potential.
- Our study screened multiple clinical prognostic factors and incorporated them into the model to establish a nomogram showing good performance for predicting the response to neoadjuvant treatment.

Neoadjuvant chemoradiotherapy treatment

All enrolled patients received standard nCRT, either mFOLFOX6 (oxaliplatin 85 mg/m^2, intravenous drip over 2 h on day 1; calcium folinate 200 mg/m^2, intravenous drip over 2 h on day 1, 5 FU 400 mg/m^2 intravenous drip, day 1, 5 FU 1200 mg/m^2 continuously for 46–48 h, repeated every 2 weeks, 28 days as one cycle) or CapeOX (capecitabine 1000 mg/m^2, orally, bid, days 1–14, oxaliplatin 130 mg/m^2, intravenous drip, day 1, 21 days as one cycle). Radiotherapy was added to chemotherapy by concomitantly using three-dimensional conformal intensity-modulated radiotherapy (total dose of 45–50.4 Gy), 5 days/week for 5 weeks with a daily fraction of 1.8–2.0 Gy. Total mesorectal excision was completed 6–8 weeks after the completion of nCRT.

Preoperative evaluation and evaluation of the efficacy of nCRT

Age, sex, distance from the anal margin, circumferential resection margin, extramural venous invasion, peripheral degree, tumor diameter, carcinoembryonic antigen (CEA), carbohydrate antigen 19-9 (CA19-9), and TNM stages were extracted from the medical records, MRI, and digital rectal examination. Postoperative specimens were evaluated by pathological assessment according to the standard Manderd system TRG (12): 1) TRG 1, no residual tumor cell; 2) TRG 2, tumor regression is obvious, only scattered single tumor cells or small nests of tumor; 3) TRG 3, tumor tissue with obvious fibrous necrosis accounting for more than 50%; 4) TRG 4, the tumor slightly subsided, the residual tumor cells exceed the inflammation area of fibrous necrosis; and 5) TRG 5, no change at all. TRG 1/2, was considered as a good response to nCRT and belonged to the nCRT-sensitive group, while TRG 3/4/5 belonged to the nCRT-resistance group. A radiomics label was added according to this classification (13).

MRI

All patients were scanned with a 3.0 T superconducting MRI scanner (Verio syngo, Siemens) with an 8-channel array. All patients underwent rectal dynamic-contrast MRI protocol. The MRI parameters were as follows: 1) Axial T2-weighted imaging: repetition time (TR) 2000 ms, echo time (TE) 101 ms, field of view (FOV) 640×640 mm, matrix 256×320, layer thickness 4 mm. 2) Sagittal T2-weighted imaging: TR 3500 ms, TE 116 ms, FOV 360×360 mm, matrix 256×320, layer thickness 3 mm. 3) Contrast-enhanced axial T1-weighted imaging: TR 5.21 ms, TE 1.76 ms, matrix 640×432, FOV 192×192 mm, slice thickness 4.0 mm, a total of 30 phases. Gadobutrol was injected at rate 3 mL/s, and the dose was 0.1 mmol/kg. The contrast was scanned at 120 s for a total scan time of 300 s.

Data processing

All the MRI images were obtained from the picture archiving and communication system (PACS, Neusoft, version 5.5.5.70228). The reprocessing of the images was performed using standardization: (gray value - average value)/standard deviation. The images were examined and segmented using ITK-snap (version 3.6.0, www.itk-snap.org) that was run independently by two radiologists with 13 and 15 years of experience, respectively. If a divergence occurred during segmentation, other senior radiologists were invited. The region of interest (ROI) was delineated layer by layer along the edge of the lesion, avoiding air-containing cavities.

Radiomics feature extraction and selection

The radiomics signature included 30 image features derived from axial contrast-enhanced T1-weighted and sagittal T2-weighted images (Supplementary Table S1), including gray-level co-occurrence matrix (GLCM), gray-level size zone matrix (GLSZM), gray-level run-length matrix (GLRLM), and neighborhood gray-tone difference matrix (NGTDM) (14) and were extracted using Matlab 2018a from 3D images. The intraclass correlation coefficient (ICC) was calculated using 50 randomly chosen images to estimate feature robustness with a cutoff value of 0.85. For machine learning classifiers, the selected features were treated with the minimum redundancy maximum relevance (mRMR) algorithm and remained the top 1% ranked features as the inputs. For radiomics nomogram methods,

the features were further selected with univariable logistic regression, followed by the least absolute shrinkage and selection operator (LASSO) logistic regression so as to obtain predictive features and to exclude relevant but redundant features (15).

Machine learning methods

To predict the therapeutic responses, three machine learning algorithms were used, including random forest (RF), support vector machine (SVM), and k-nearest neighbors (KNN). We also proposed an ensemble classifier (EC) in order to integrate the outputs from those three models. The final output of the EC was calculated as $P = (p1 + p2 + p3) / 3$, where $p1$, $p2$ and $p3$ were the output from three RFs. The machine learning classifiers were all implemented in Matlab 2018a.

Construction of the radiomics nomogram

The radiomics signature was calculated by a linear combination of selected features weighted by the respective LASSO coefficients. Multivariable logistic regression was used to evaluate the significant clinical factors for prediction of the therapeutic response to nCRT, followed by backward stepwise selection with Akaike's information criterion (AIC) as the stopping rule (16). The radiomics score was calculated by combining the radiomics signature and the selected preoperative clinical parameters. A radiomics nomogram was constructed on the basis of the multivariable logistic analysis using an 'rms' package in the R language (v. 3.5.0; https://www.r-project.org).

Validation strategy

To evaluate the performance of the radiomics methods, 10-fold cross-validation was used. Prediction accuracy, sensitivity, and specificity were calculated (17). To validate the radiomics nomogram, the logistic regression formula that was formed from the training group was applied to the validation group. The radiomics scores were calculated for each patient. A calibration curve was plotted to assess the nomogram. Decision curve analysis (DCA) was also conducted to assess the clinical usefulness of the nomogram model by calculating the net benefits for a range of threshold probabilities in the training and validation group.

Statistical analysis

Statistical analysis was conducted using the R software (v. 3.5.0; https://www.r-project.org). The packages in R that were used in this study are reported in the construction of radiomics nomogram, above. Normally distributed data were presented as means ± standard deviation (SD). While, non-normally distributed variables were presented as median (minimum–maximum) according to the results of the Kolmogorov–Smirnov test for normal distribution. Normally distributed data were analyzed using t-test. Non-continuous data were presented as frequency and percentage which were analyzed by chi-square test or Fisher Freeman Halton test, as appropriate. The receiver operating characteristic (ROC) analysis was performed by plotting the sensitivity versus specificity to describe the performance of the methods. Area under the curve (AUC) values were calculated to quantify the discrimination performance. The reported statistical significance levels were all two-sided, with statistical significance set at 0.05.

Results

A total of 189 patients with LARC (53 male and 136 female; mean age, 60.5 years; range, 34–78 years) were enrolled. Supplementary Fig. S1 shows images from MRI scans of two exemplary patients, with ROIs segmented by the radiologists. Both patients were treated with nCRT; one had a good therapeutic response (Supplementary Fig. S1a–d), and the other had a poor therapeutic response (Supplementary Fig. S1e–h). No significant differences were observed following a visual inspection by radiologists.

The characteristics of the patients in both the training and validation groups are shown in Table 1. In the training set (n=134), there were 54 nCRT-resistant and 80 nCRT-sensitive patients. In the validation set (n=55), there were 22 nCRT-resistant and 33 nCRT-sensitive patients. In both cohorts, tumor size and CEA levels were larger in the nCRT-resistant subgroups, while CA19-9 levels were lower (all $p < 0.05$). In the training cohort, extramural venous invasion was

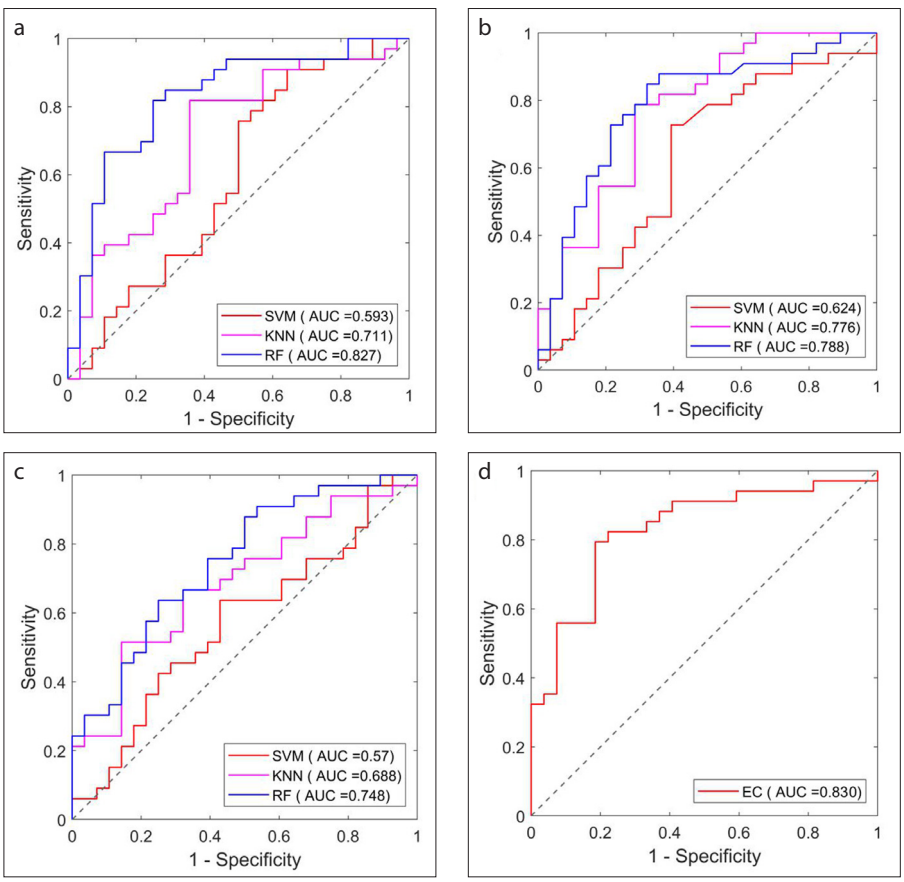

Figure 1. a-d. ROC curves for the machine learning classifiers: **(a)**, ROC curve for the three classifiers on sagittal T2-weighted imaging; **(b)**, ROC curve for the three classifiers on axial contrast-enhanced T1-weighted imaging; **(c)**, ROC curve for the three classifiers on axial T2-weighted imaging; **(d)**, ROC curve for the ensemble classifier combing outputs from three RFs using axial T2-weighted imaging, axial contrast-enhanced T1-weighted imaging, and sagittal T2-weighted imaging, respectively.

Table 1. Characteristics of patients with LARC in training and validation cohorts

Characteristics	Training cohort (n=134)			Validation cohort (n=55)		
	nCRT-sensitive (n=80)	nCRT-resistant (n=54)	*p*	nCRT-sensitive (n=33)	nCRT-resistant (n=22)	*p*
Age (years), mean±SD	58.82±9.35	58.78±9.37	0.543	59.86±9.79	60.07±9.49	0.800
Sex, n (%)			0.930			0.116
Male	17 (22.67)	13 (22.03)		15 (51.72)	8 (30.77)	
Female	58 (77.33)	46 (77.97)		14 (48.28)	18 (69.23)	
Distances from the anal margin, n (%)			0.770			0.760
>5 cm	22 (29.33)	26 (44.07)		5 (17.24)	10 (38.46)	
≤5 cm	53 (70.67)	33 (55.93)		24 (82.76)	16 (61.54)	
Tumor-axis diameter (cm), mean±SD	5.46±3.27	6.35±4.51	0.031[a]	5.79±2.67	7.15±1.51	<0.001[a]
CEA, n (%)			<0.001[a]			<0.001[a]
≤5 ng/mL (normal)	63 (84)	6 (10.17)		27 (93.10)	2 (7.69)	
>5 ng/mL (abnormal)	12 (16)	53 (89.83)		2 (6.90)	24 (92.31)	
CA19-9, n (%)			<0.001[a]			0.001[a]
≤35 U/mL (normal)	8 (10.67)	36 (61.02)		3 (10.34)	15 (57.69)	
>35 U/mL (abnormal)	67 (89.33)	23 (38.98)		26 (89.66)	11 (42.31)	
Peripheral degree, n (%)			0.186			0.085
≤75%	69 (92.00)	50 (84.75)		27 (93.10)	20 (76.92)	
>75%	6 (8.00)	9 (15.25)		2 (6.90)	6 (23.08)	
CRM status, n (%)			0.050			0.385
+	10 (13.33)	20 (33.90)		5 (17.24)	7 (26.92)	
-	65 (86.67)	39 (66.10)		24 (82.76)	19 (73.08)	
EMVI status, n (%)			0.016a			0.171
+	11 (14.67)	20 (33.90)		2 (6.90)	5 (19.23)	
-	64 (85.33)	39 (66.10)		27 (93.10)	21 (80.77)	
T stages, n (%)			0.871			0.019[a]
T3	20 (26.67)	15 (25.42)		13 (44.83)	4 (15.38)	
T4	55 (73.33)	44 (74.58)		16 (55.17)	22 (84.62)	
N stages, n (%)			0.846			0.161
N0	31 (41.33)	28 (47.46)		19 (65.52)	11 (42.31)	
N1	26 (34.67)	14 (23.73)		3 (10.34)	7 (26.92)	
N2	18 (24.00)	17 (28.81)		7 (24.14)	8 (30.77)	
M stages, n (%)			0.004[a]			0.493
M0	73 (97.33)	49 (83.05)		28 (96.55)	24 (92.31)	
M1	2 (2.67)	10 (16.95)		1 (3.45)	2 (7.69)	
Neoadjuvant therapy, n (%)			0.631			0.771
mFolfox6+IMRT	38 (50.67)	30 (50.85)		16 (55.17)	15 (57.69)	
CapeOX+IMRT	37 (49.33)	29 (49.15)		13 (44.83)	11 (42.31)	

p values were calculated from the univariate association analyses between the TRG outcomes and each clinical factor.
LARC, locally advanced rectal cancer; nCRT, neoadjuvant chemoradiotherapy; SD, standard deviation; CEA, carcinoembryonic antigen; CA19-9, carbohydrate antigen 19-9; Peripheral degree, the extent of invasion of the intestinal wall by rectal cancer; CRM, circumferential resection margin; EMVI, extramural venous invasion; IMRT, intensity-modulated radiotherapy.
[a]$p < 0.05$.

lower in the nCRT-resistant subgroup, while the M1 status was higher (all $p < 0.05$). In the validation cohort, the T stages were higher ($p = 0.019$).

Table 2 gives the performance of each feature set and machine learning classifier, and the performance of the ROC analyses for the machine learning classifiers is shown in Fig. 1. RF was better than SVM and KNN among the three machine learning algorithms (Fig. 1a–1c). The ensembled classifier combing outputs from three RFs had

the highest prediction performance (AUC= 0.830) (Table 2 and Fig. 1d).

The nomogram integrating the axial contrast-enhanced T1-weighted imaging, sagittal T2-weighted imaging, CEA, and tumor diameter (Fig. 2a) showed good agreements according to the calibration curves in the training and validation groups (Fig. 2b, 2c). The ROC curves (Fig. 2d, 2e) showed good performance of the radiomics nomogram in the training and validation groups with AUCs of 0.970 (95% CI, 0.942–0.997; sensitivity, 0.939; specificity, 0.898) and 0.949 (95% CI, 0.892–1.000; sensitivity, 0.879; specificity, 0.909), respectively.

The radiomics nomogram yielded the greatest AUC of 0.949 in the validation group by integrating both the MRI features and the clinical parameters, which achieved better predictive efficacy compared with using only the image features from pre-treatment MRI (AUC=0.749).

Table 2. Performance of the machine learning classifiers with different MRI datasets

Classifiers/MRI datasets	AUC	ACC (%)	SEN	SPE	*p*
RF/T1WI C+	0.827	73.770	0.818	0.750	<0.001
RF/T2WI axial	0.748	65.574	0.636	0.750	<0.001
RF/T2WI sagittal	0.788	70.492	0.848	0.679	<0.001
KNN/T1WI C+	0.711	73.770	0.818	0.643	0.009
KNN/T2WI axial	0.688	67.213	0.515	0.857	0.023
KNN/T2FS sagittal	0.776	73.770	0.788	0.714	0.004
SVM/T1WI C+ axial	0.593	62.295	0.909	0.357	0.121
SVM/T2WI axial	0.570	52.459	0.636	0.571	0.217
SVM/T2FS sagittal	0.624	59.016	0.727	0.607	0.089
EC/(T1WI C+ axial +T2WI axial +T2WI sagittal)	0.830	75.410	0.794	0.815	<0.001

MRI, magnetic resonance imaging; AUC, area under the curve; ACC, accuracy; SEN, sensitivity; SPE, specificity; RF, random forest; T1WI, T1-weighted imaging; T2WI, T2-weighted imaging; C+, with contrast; KNN, k-nearest neighbors; SVM, support vector machine; FS, fat suppression; EC, ensembled classifier.

The decision curve to estimate the clinical utility of the nomogram (Fig. 3) showed that the nomogram for predicting therapeutic response would be more beneficial if the patients' threshold probability was between 0.03 and 0.96, i.e., the benefit rate is above 0 when the threshold is within this range.

Discussion

In terms of current imaging technology, it is a big challenge to accurately identify the changes in the residual tumor tissue and determine the degree of invasion after nCRT (6, 18). Radiomics have been receiving increased attention over the recent years by providing nonvisual information related with tumor heterogeneity and pathophysiology through high-throughput extraction of quantitative texture features from medical images, which showed excellent performance potential in predicting tumor biological behavior, efficacy, and prognosis (19, 20). The radiomics methods for the prediction of the therapeutic response in LARC patients with nCRT proposed in this study worked well and represent a predictive tool that can be used for personalized therapies.

Machine learning-based radiomics methods for medical diagnosis and classification have been used and compared in medical

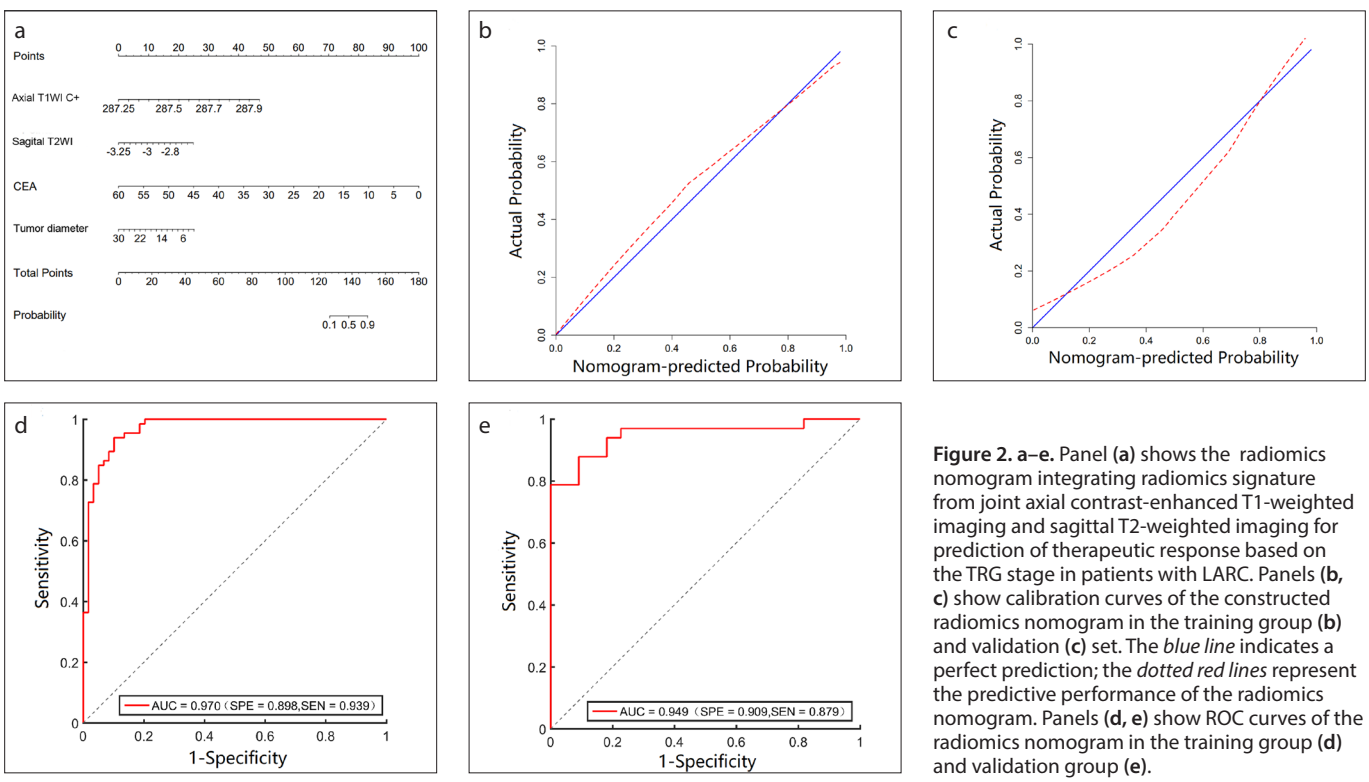

Figure 2. a–e. Panel **(a)** shows the radiomics nomogram integrating radiomics signature from joint axial contrast-enhanced T1-weighted imaging and sagittal T2-weighted imaging for prediction of therapeutic response based on the TRG stage in patients with LARC. Panels **(b, c)** show calibration curves of the constructed radiomics nomogram in the training group **(b)** and validation **(c)** set. The *blue line* indicates a perfect prediction; the *dotted red lines* represent the predictive performance of the radiomics nomogram. Panels **(d, e)** show ROC curves of the radiomics nomogram in the training group **(d)** and validation group **(e)**.

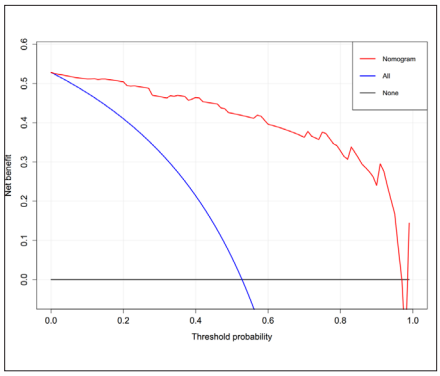

Figure 3. DCA for the constructed radiomics nomogram. The x-axis and y-axis represent the threshold probability and net benefit, respectively. The red line represents the radiomics nomogram model. The blue line indicates the assumption that all patients were nCRT-sensitive. The black line represents the hypothesis that all patients were nCRT-resistant.

images (21), integrating high-dimensional features, which can hardly be understood by radiologists with visual inspection (22). Nevertheless, there is still no uniform standard to determine which classifier is more suitable for a particular application. Our results demonstrated that the RF outperformed KNN and SVM in terms of AUCs on axial contrast-enhanced T1-weighted, axial T2-weighted, and sagittal T2-weighted images. To incorporate the outputs from MRI, we proposed an ensembled classifier that averaged the outputs from three RFs using axial contrast-enhanced T1-weighted, axial T2-weighted, and sagittal T2-weighted imaging as inputs, respectively, and obtained the highest prediction performance, which outperformed all of the single classifiers. Since the radiomics nomogram method has been frequently used over the recent years and has been shown to be effective for disease diagnosis and evaluation of prognosis by incorporating radiomics signatures and clinical factors (23), we also built and evaluated a nomogram model for comparison. Our radiomics nomogram incorporated axial contrast-enhanced T1-weighted imaging, sagittal T2-weighted imaging, CEA, and tumor diameter and showed good predictive performance with AUC of 0.970 and 0.949 in the training and validation groups, respectively, suggesting that it can be used for individualized preoperative prediction of nCRT.

The radiomics signature with clinical parameters was evaluated using multivariable logistic regression by backward stepwise selection with AIC as the stopping rule. Our results showed that the CEA and tumor diameter were independent predictors of the nCRT response, and could be included in the radiomics nomogram model. All the other clinical parameters were excluded from the nomogram model due to the low predictive power determined by the multivariable logistic regression. CEA was selected as a very important clinical factor in our nomogram model. Based on our clinical experience, CEA is a commonly used blood test for early screening and prognosis evaluation of colorectal cancer. Some previous reports suggested that this factor was highly correlated to radiotherapy responses in patients with colorectal cancer (24, 25). Our results indicated that CEA could serve as a potential marker for evaluating the therapeutic responses in LARC patients and should be given more attention in future studies. The tumor diameter of lesion was kept in the nomogram model, considering that the post-treatment data represent the current status of the tumor after nCRT, which can provide more correlative information of the pathological changes. Based on our clinical experience, the tumor diameter of the lesion has the potential to predict pathological adenocarcinoma. Nevertheless, if the tumor diameter was removed from the nomogram model, the AUC was slightly decreased in both the training (0.954 vs. 0.970) and validation (0.945 vs. 0.949) cohorts.

There has been previous attempts to use MRI data for predicting pathologic complete response. De Cecco et al. (11) evaluated the nCRT response using texture analysis methods; however, their research lacked clinical significance since only 15 patients were enrolled. Nie et al. (26) reported on predicting the power of pathologic complete response outcomes in LARC patients using dynamic contrast-enhanced (DCE) MRI and diffusion-weighted imaging (DWI) and established an artificial neural network model. Yet, the long scanning time for DCE MRI and DWI, as well as the complex post-processing steps of the scanned images, hindered the clinical applications of the model. Our proposed radiomics nomogram model combined only two pre-treatment MRI sequences (axial contrast-enhanced T1-weighted and sagittal T2-weighted imaging) and two clinical parameters, thus making it a powerful and easy-to-use discriminative tool with potential clinical applicability.

There are some limitations to the present study. First, the enrolled patients were all from a single hospital, which may lead to biased results. Second, the sample size was still relatively small. Future studies should use larger datasets from multiple centers. In addition, the application of our proposed nomogram model still requires tedious manual operations like handcrafted segmentation of tumor regions. We assume that automated analysis could be achieved by deep-learning based radiomics models, which will be addressed in our future work.

In conclusion, our work investigated and validated radiomics methods for the prediction of the therapeutic responses to nCRT in LARC patients using multiple MRI sequences, which could be potentially used in assisting future clinical applications.

Conflict of interest disclosure

The authors declared no conflicts of interest.

References

1. Siegel RL, Miller KD, Jemal A. Cancer statistics, 2018. CA: a cancer journal for clinicians 2018; 60:277–300. [Crossref]
2. Torre LA, Siegel RL, Ward EM, Jemal A. Global cancer incidence and mortality rates and trends--an update. Cancer Epidemiol Biomarkers Prev 2016; 25:16–27. [Crossref]
3. Ludmir EB, Palta M, Willett CG, Czito BG. Total neoadjuvant therapy for rectal cancer: An emerging option. Cancer 2017; 123:1497–1506. [Crossref]
4. Peng YF, Yu WD, Pan HD, et al. Tumor regression grades: potential outcome predictor of locally advanced rectal adenocarcinoma after preoperative radiotherapy. World J Gastroenterol 2015; 21:1851–1856. [Crossref]
5. Vecchio FM, Valentini V, Minsky BD, et al. The relationship of pathologic tumor regression grade (TRG) and outcomes after preoperative therapy in rectal cancer. Int J Radiat Oncol Biol Phys 2005; 62:752–760. [Crossref]
6. Bouzourene H, Bosman FT, Seelentag W, Matter M, Coucke P. Importance of tumor regression assessment in predicting the outcome in patients with locally advanced rectal carcinoma who are treated with preoperative radiotherapy. Cancer 2002; 94:1121–1130. [Crossref]
7. Sclafani F, Brown G, Cunningham D, et al. Comparison between MRI and pathology in the assessment of tumour regression grade in rectal cancer. Br J Cancer 2017; 117:1478–1485. [Crossref]
8. Tapan U, Ozbayrak M, Tatli S. MRI in local staging of rectal cancer: an update. Diagn Interv Radiol 2014; 20:390–398. [Crossref]
9. Aerts HJ, Grossmann P, Tan Y, et al. Defining a radiomic response phenotype: a pilot study using targeted therapy in NSCLC. Sci Rep 2016; 6:33860. [Crossref]
10. Hodgdon T, McInnes M D, Schieda N, Flood TA, Lamb L, Thornhill RE. Can quantitative CT texture analysis be used to differentiate fat-poor renal angiomyolipoma from renal cell carcinoma on unenhanced CT images? Radiology 2015; 276:787–796. [Crossref]

11. De Cecco CN, Ganeshan B, Ciolina M, et al. Texture analysis as imaging biomarker of tumoral response to neoadjuvant chemoradiotherapy in rectal cancer patients studied with 3-T magnetic resonance. Invest Radiol 2015; 50:239–245. [Crossref]
12. Mandard AM, Dalibard F, Mandard JC, et al. Pathologic assessment of tumor regression after preoperative chemoradiotherapy of esophageal carcinoma. Clinicopathologic correlations. Cancer 2015; 73:2680–2686.
13. Santos M D, Silva C, Rocha A, Matos E, Nogueira C, Lopes C. Tumor regression grades: can they influence rectal cancer therapy decision tree?. Int J Surg Oncol 2013; 2013:572149. [Crossref]
14. Aerts H J, Velazquez E R, Leijenaar R T, et al. Decoding tumour phenotype by noninvasive imaging using a quantitative radiomics approach. Nat Commun 2014; 5:4006. [Crossref]
15. Sauerbrei W, Royston P, Binder H. Selection of important variables and determination of functional form for continuous predictors in multivariable model building. Stat Med 2010; 26:5512–5528. [Crossref]
16. Collins G S, Reitsma J B, Altman D G, Moons K G. Transparent reporting of a multivariable prediction model for individual prognosis or diagnosis (TRIPOD): the TRIPOD statement. Eur Urol 2015; 102:148–158. [Crossref]
17. Zhou Y, Xu J, Liu Q, et al. A radiomics approach with CNN for shear-wave elastography breast tumor classification. IEEE Trans on Biomed Eng 2018; 65:1935–1942. [Crossref]
18. Seierstad T, Hole KH, Groholt KK, et al. MRI volumetry for prediction of tumour response to neoadjuvant chemotherapy followed by chemoradiotherapy in locally advanced rectal cancer. Br J Radiol 2015; 88:20150097. [Crossref]
19. Gillies R J, Kinahan P E, Hricak H. Radiomics: images are more than pictures, they are data. Radiology 2016; 278:563–577. [Crossref]
20. Liu Z, Zhang X Y, Shi Y J, et al. Radiomics analysis for evaluation of pathological complete response to neoadjuvant chemoradiotherapy in locally advanced rectal cancer. Clin Cancer Res 2017; 23:7253–7262. [Crossref]
21. Wang J, Wu CJ, Bao ML, Zhang J, Wang XN, Zhang YD. Machine learning-based analysis of MR radiomics can help to improve the diagnostic performance of PI-RADS v2 in clinically relevant prostate cancer. Eur Radiol 2017; 27:4082–4090. [Crossref]
22. Wang H, Zhou Z, Li Y, et al. Comparison of machine learning methods for classifying mediastinal lymph node metastasis of non-small cell lung cancer from (18)F-FDG PET/CT images. EJNMMI Res 2017; 7:11. [Crossref]
23. Ezuddin NS, Pretell-Mazzini J, Yechieli RL, Kerr DA, Wilky BA, Subhawong TK. Local recurrence of soft-tissue sarcoma: issues in imaging surveillance strategy. Skeletal Radiol 2018; 47:1595–1606. [Crossref]
24. Kleiman A, Al-Khamis A, Farsi A, et al. Normalization of CEA levels post-neoadjuvant therapy is a strong predictor of pathologic complete response in rectal cancer. J Gastrointest Surg 2015; 19:1106–1112. [Crossref]
25. Zhang ZY, Gao W, Luo QF, et al. A nomogram improves AJCC stages for colorectal cancers by introducing CEA, modified lymph node ratio and negative lymph node count. Sci Rep 2016; 6:39028. [Crossref]
26. Nie K, Shi L, Chen Q, et al. Rectal cancer: assessment of neoadjuvant chemoradiation outcome based on radiomics of multiparametric MRI. Clin Cancer Res 2016; 22:5256–5264. [Crossref]

Supplementary Table S1. Radiomics features extracted from axial contrast-enhanced T1-weighted and sagittal T2-weighted MRI

Types	Radiomics feature
Gray-Level Co-occurrence Matrix (GLCM)	Autocorrelation, ClusterTendency, ClusterProminence , Correlation, SumSquares, DifferenceEntropy, Idn, ClusterShade, Idmn, Imc1, InverseVariance, DifferenceAverage
Gray Level Size Zone Matrix (GLSZM)	LargeAreaEmphasis, GrayLevelNonUniformity, SmallAreaHighGrayLevelEmphasis, LargeArea-HighGrayLevelEmphasis, LargeAreaLowGrayLevelEmphasis, SizeZoneNonUniformityNormalized, SmallAreaLowGrayLevelEmphasis
Gray-Level Run Length Matrix (GLRLM)	LongRunLowGrayLevelEmphasis, LongRunHighGrayLevelEmphasis, LongRunEmphasis, ShortRunEmphasis, LongRunEmphasis, GrayLevelNonUniformity
Neighborhood Gray-tone Difference Matrix (NGTDM)	Complexity, Busyness, Coarseness, Contrast, Strength

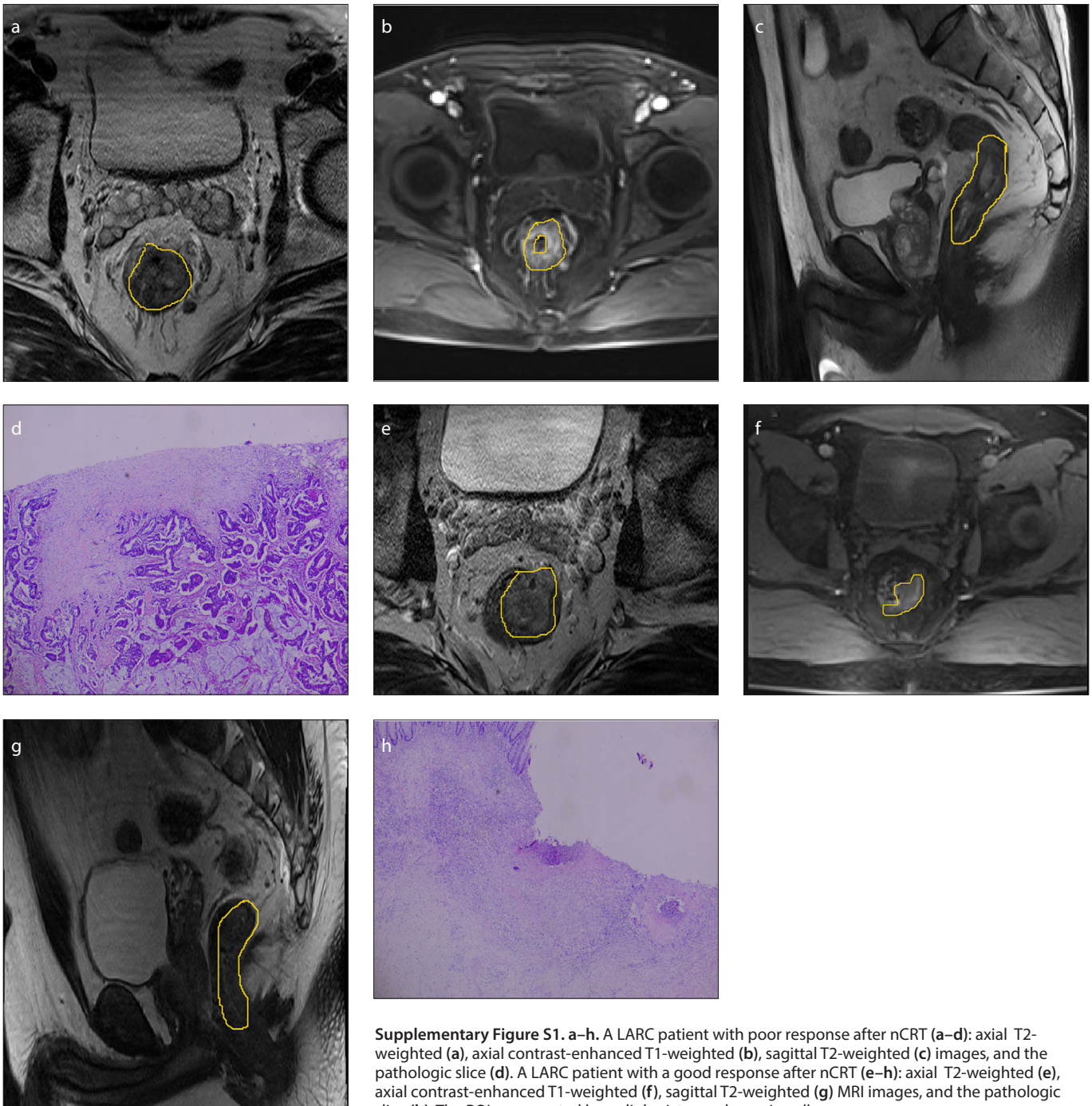

Supplementary Figure S1. a–h. A LARC patient with poor response after nCRT (**a–d**): axial T2-weighted (**a**), axial contrast-enhanced T1-weighted (**b**), sagittal T2-weighted (**c**) images, and the pathologic slice (**d**). A LARC patient with a good response after nCRT (**e–h**): axial T2-weighted (**e**), axial contrast-enhanced T1-weighted (**f**), sagittal T2-weighted (**g**) MRI images, and the pathologic slice (**h**). The ROIs segmented by radiologists are shown in *yellow*.